



Effect of fracture orientation on detection accuracy of vertical root fractures in non-endodontically treated teeth using cone beam computed tomography

Xiao-Long Guo¹ · Gang Li¹ · Shuang Yin¹ · Ruo-Han Ma¹ · Yu-Jiao Guo¹ · Michael M. Bornstein²

Received: 28 December 2018 / Accepted: 4 April 2019 / Published online: 13 April 2019
© Springer-Verlag GmbH Germany, part of Springer Nature 2019

Abstract

Objectives This study aimed to investigate the effect of fracture orientation on the detection accuracy of vertical root fractures (VRFs) in non-endodontically treated teeth using four different cone beam computed tomography (CBCT) units.

Materials and methods Thirty eight out of 148 extracted human permanent teeth were chosen randomly, and VRFs were artificially induced to result in 20 mesiodistally and 18 buccolingually oriented root fractures. The fracture width was subsequently measured. All the teeth were scanned with four CBCT units. CBCT images were evaluated independently by two observers. Area under the receiver operating characteristic curve (AUC), sensitivity, and specificity were calculated for each observer and fracture orientation. The AUC between the two fracture orientations was compared using *Z* test.

Results The mean fracture width was 140 μm (standard deviation 26.8 μm). A statistically significant difference was found between the mesiodistal and buccolingual VRFs for the AUC from the CBCT unit 3D Accuitomo 170 ($p = 0.02$). There were no statistically significant differences between the mesiodistal and buccolingual VRFs for AUCs from the CBCT units NewTom VGi ($p = 0.21$), ProMax 3D Mid ($p = 0.23$), and i-CAT FLX ($p = 0.21$).

Conclusion Fracture orientations of teeth with VRFs in non-endodontically treated teeth may play a role in the detection accuracy of CBCT images, but this effect seems to be dependent on the CBCT unit used.

Clinical relevance Although for most of the CBCT units tested, the fracture orientation of VRF in non-endodontically treated teeth seems not to play a role for the diagnosis, clinical data is needed to further assess the impact of different devices on VRF detection.

Keywords Vertical root fracture · Cone beam computed tomography · Fracture orientation · Non-endodontically treated tooth · Diagnosis

Introduction

In a vertical root fracture (VRF), the complete or incomplete fracture line is longitudinally oriented and may originate from

any level of the root and extend coronally towards the cervical margin [1]. A VRF in non-endodontically treated teeth is not uncommon in the Chinese population, with over 40% of the fractures occurring in non-endodontically treated teeth [2, 3].

✉ Gang Li
kqgang@bjmu.edu.cn

Xiao-Long Guo
robert108105147@126.com

Shuang Yin
15201278345@163.com

Ruo-Han Ma
525943920@qq.com

Yu-Jiao Guo
amberring@126.com

Michael M. Bornstein
bornst@hku.hk

¹ Department of Oral and Maxillofacial Radiology, Peking University School and Hospital of Stomatology, 22 Zhongguancun Nandajie, Haidian District, Beijing 100081, China

² Oral and Maxillofacial Radiology, Applied Oral Sciences, Faculty of Dentistry, Prince Philip Dental Hospital, The University of Hong Kong, Sai Ying Pun, Hong Kong, SAR, China

These may be due to a trauma related to certain diet patterns or chewing habits such as the chewing of bones in meat [2–5], and to the morphology such as protruding crowns and delicate root morphologies [4]. Teeth with VRFs often lead to the development of a deep osseous defect around the fracture site [6], and resorption of the fractured root has also been reported [7]. Therefore, a timely and definite diagnosis is important to avoid progressive alveolar bone loss, which may make future restorative procedures difficult [8].

The diagnosis of VRFs can be challenging for the lack of specific clinical signs, symptoms, and/or radiographic features [9]. An important aspect for the definite diagnosis includes radiographic demonstration of a fracture line or even lines [10]. Periapical radiography has limitations in the detection of VRFs, especially when the fracture plane is located in a mesiodistal direction [11–14]. This is mainly due to superimposition of adjacent structures and the difficulty that the primary beam needs to be aligned with the fracture plane [15–18]. In the literature, it has been stated that periapical radiography can detect about one third of the VRFs [19].

Cone beam computed tomography (CBCT) is reported to have higher accuracy than periapical radiography in the detection of VRFs in non-endodontically treated teeth [20, 21]. However, the detection accuracy of VRFs in non-endodontically treated teeth using CBCT varies from study to study [22–26]. Fracture characteristics such as the fracture orientation of the VRF in teeth with intra-canal metal post have been reported to play a role in the detection accuracy using CBCT [13]. However, whether the fracture orientation has an effect on the detection accuracy of VRFs in non-endodontically treated teeth has not been reported yet. Therefore, the objective of the present study is to investigate the influence of fracture orientation in the detection accuracy of VRFs in non-endodontically treated teeth using four different CBCT units.

Materials and methods

Sample preparation

This study was approved by the Institutional Review Board of Peking University School and Hospital of Stomatology (PKUSSIRB-201838111). One-hundred and forty-eight human permanent teeth (12 anterior teeth, 125 premolars, and 11 mandibular molars) were obtained without information on age and sex from the Department of Oral and Maxillofacial Surgery, Peking University School and Hospital of Stomatology. The majority of the teeth (premolars) were from young orthodontic patients, and the remaining teeth (anterior teeth and molars) were mainly from patients experiencing tooth loss due to severe periodontitis. Soft tissue and calculus on teeth were removed. Teeth with caries involving the roots,

external root resorption, extremely curved roots, and open apices were not included. Periapical radiographs were taken to exclude teeth with calcified root canal(s), internal root resorption, complex root canal morphologies, and endodontically treated teeth. Teeth were evaluated with a magnifying glass ($\times 2$) to exclude root fracture. If root fractures were suspected, a three-dimensional laser scanning microscope (VK-X100/X200, Keyence, Japan) was used for confirmation. The teeth were stored in normal saline except during VRF induction and CBCT scanning.

Thirty-eight teeth were randomly chosen from the 148 teeth for VRF induction. In 18 teeth, fractures in the buccolingual direction and in 20 teeth in the mesiodistal direction were made with the following procedure. The teeth were fixed with paraffin wax, with their longitudinal root axes parallel to the platform of a diamond-coated wire saw machine (STX-202AQ, MTI Corp., China). Then, the teeth were cut into two halves with a diamond-coated wire of 0.25-mm diameter (Fig. 1a). The two halves from the same tooth were then repositioned with cyanoacrylate adhesive.

Fracture width measurement

Six out of the 38 VRF teeth were chosen randomly and scanned with the Inveon Micro-CT (Siemens, Munich, Germany) with an 8.89- μm resolution. The scan parameters were 80 kV, 500 μA , acquisition time 13.8 min, and a field of view of 18.2 (trans-axial) \times 27.3 (axial) mm. The fracture width was determined on one Micro-CT cross-sectional image in the midpoint of each third of the fractured roots (Fig. 1b). The maximum width obtained from the three cross-sectional images was recorded as the width of fracture.

CBCT image acquisition

Dry human mandibles were borrowed from the Department of Human Anatomy and Histology and Embryology, Peking University Health Science Center. All teeth were coded and allocated randomly into one of 7 dry human mandibles (Fig. 1c). Each mandible was used twice, which equals to 14 mandibles in total. According to the sockets available, each mandible contained 7 to 14 teeth, including both VRF teeth and control teeth, and the number of VRF teeth in each mandible was randomized. In each mandible, teeth were fitted into a relatively suitable socket by one investigator, who was not involved in the image evaluation. The gap between the root and socket wall was filled with paraffin wax to simulate the radiographic aspect of the periodontal ligament space and to keep the teeth stable. The mandibles were then placed into a cylindrical 20-mm-thick water phantom to simulate soft tissues [27]. The water phantom was placed on the chinrest platform or chair of each CBCT unit, with the occlusion plane

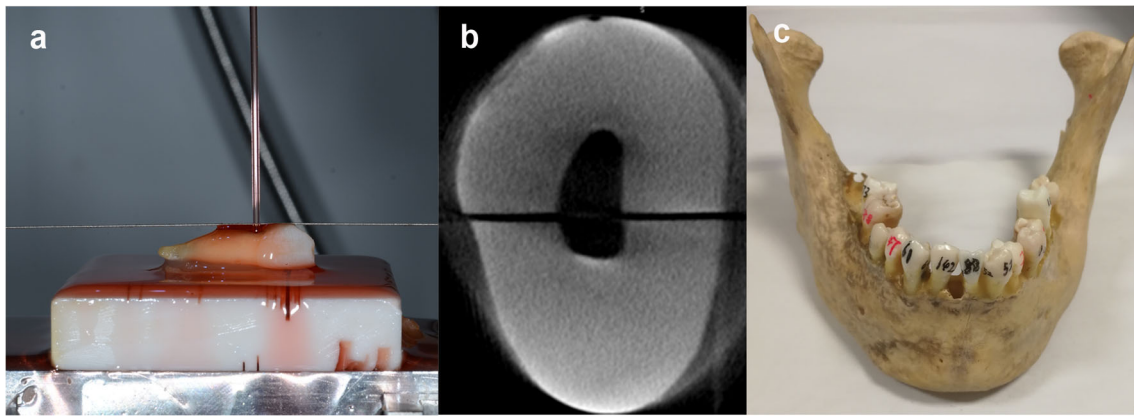


Fig. 1 Sample preparation. **a** Vertical root fracture induction. **b** Fracture width measurement on an axial micro-CT image. **c** One of the 7 dry human mandibles with 13 teeth (including teeth both with and without vertical root fractures) placed inside the sockets

parallel to the horizontal plane and the mandible in the center of the scanned field of view.

The CBCT units used were NewTom VGi (Quantitative Radiology, Verona, Italy), ProMax 3D Mid (Planmeca Oy, Helsinki, Finland), 3D Accuitomo 170 (J Morita Mfg., Corp., Kyoto, Japan), and i-CAT FLX (Imaging Sciences International Inc., Hatfield, PA). The exposure parameters used for each CBCT unit are presented in Table 1. After image acquisition, all images were reconstructed with the dedicated software from each CBCT unit. The thickness of the axial images from all CBCT units was the smallest thickness available for each CBCT, which is 0.15 mm for the ProMax 3D Mid and 0.125 mm for the other three CBCT units. These were all kept for the following observations. A total of 78 CBCT datasets were created, including 25 for both NewTom VGi and 3D Accuitomo 170, and 14 for both ProMax 3D Mid and i-CAT FLX. The reason why the number of datasets from the NewTom VGi and 3D Accuitomo 170 were 25 rather than 14 is because of the relatively small field of view used for the scan. Thus, only one side of the mandible was scanned each time except for two mandibles.

CBCT image evaluation

Two oral and maxillofacial radiology residents with at least 3 years of experience in CBCT image interpretation evaluated all radiographs separately. Observers were blinded to the

status of the teeth. However, they were aware of the fact that certain teeth were without root fractures. Prior to the actual assessment, the observers were calibrated by providing and training them with typical radiographic features of VRFs. The CBCT data from teeth used for calibration were not included in the later evaluation. Also, the observers were required to view the axial, coronal, and sagittal tomographic slices using the proprietary software of each CBCT unit. All 78 CBCT datasets were numbered from 1 to 78. To avoid viewing fatigue, the images were randomly divided into 4 groups and at each time only one group of images was assessed irrespective of the CBCT used.

The observers classified the presence of VRF by using a 5-point scale as follows: (1) definitely absent, (2) probably absent, (3) unsure, (4) probably present, and (5) definitely present. All images were displayed on a 14-in. ThinkPad T450 monitor (Lenovo, Beijing, China) in a quiet room under dimmed ambient light. The brightness, contrast, and zoom tools were allowed to adjust. There was no time restriction for an observation. The main radiographic feature for a present VRF was defined as a direct radiolucent line crossing the trunk of the root in at least two consecutive sections on any of the three slices [11]. A second evaluation was performed under the same conditions with 20% of the randomly selected sample teeth after 2 weeks by the two observers to assess the intra-observer agreement.

Table 1 Exposure parameters used for each CBCT unit in the present study

	FOV (diameter × height) (mm ²)	Voxel size (μm)	Tube voltage (kVp)	Tube current (mA)	Scan time (s)
NewTom VGi	60 × 60	125	110	1~3.65	36
ProMax 3D Mid	80 × 80	150	90	10	15
3D Accuitomo 170	60 × 60	125	90	5	30.8
i-CAT FLX	80 × 80	125	120	5	26.9

FOV field of view

Statistical analysis

Data analysis was conducted using the SPSS software, version 17.0 (SPSS Inc., Chicago, IL), and a significance level of 5% was set. To determine the overall diagnostic accuracy, the receiver operating characteristic (ROC) curve was constructed through the MedCalc Statistical Software version 15.2.2 (MedCalc Software bvba, Ostend, Belgium; <http://www.medcalc.org>; 2015). Scores from the two observers were combined to generate a pooled ROC curve for each fracture orientation. To calculate the sensitivity and specificity for the two fracture orientations, the observers' responses were dichotomized into the presence or absence of fractures. Scores of 1, 2, and 3 were regarded as fracture absence; scores of 4 and 5 were considered fracture presence. The areas under the ROC curves (AUCs) were compared between the two fracture orientations within each CBCT unit using Z test for two independent ROC curves. Based on the 95% confidence interval, the differences between the two fracture orientations for sensitivity and specificity were tested. Intra- and inter-observer agreement was assessed for the two observers using the weighted Cohen kappa test.

Results

The mean fracture width of the included teeth with a VRF was 140 μm (standard deviation 26.8 μm), and the fracture widths

Table 2 Intra- and inter-observer kappa values regarding VRF detection for each of the four CBCT units

	Intra-observer kappa	Inter-observer kappa
NewTom VGi	0.89	0.84
ProMax 3D Mid	0.56	0.58
3D Accuitomo 170	0.77	0.76
i-CAT FLX	0.80	0.66

Kappa values: agreement was rated as “low” (< 0.41), “moderate” (0.41–0.60), “substantial” (0.61–0.80), and “excellent” (> 0.80)

were ranging from 110 to 170 μm . An example of representative axial CBCT images of teeth with VRFs from the four different CBCT units used is shown in Fig. 2.

The intra- and inter-observer kappa values in the detection of VRFs from the four CBCT units are shown in Table 2. The intra- and inter-observer agreement was excellent for the CBCT unit NewTom VGi, while for the ProMax 3D Mid the intra- and inter-observer agreement was moderate.

The sensitivity, specificity, and AUC for the mesiodistal and buccolingual VRFs from the four CBCT units for each observer are presented in Table 3. Generally, there are no statistically significant differences between the detection of buccolingual and mesiodistal VRFs except for the CBCT images scanned with 3D Accuitomo 170. For this device, the detection accuracy for teeth with a mesiodistal VRF is lower than that for teeth with a buccolingual VRF. Receiver

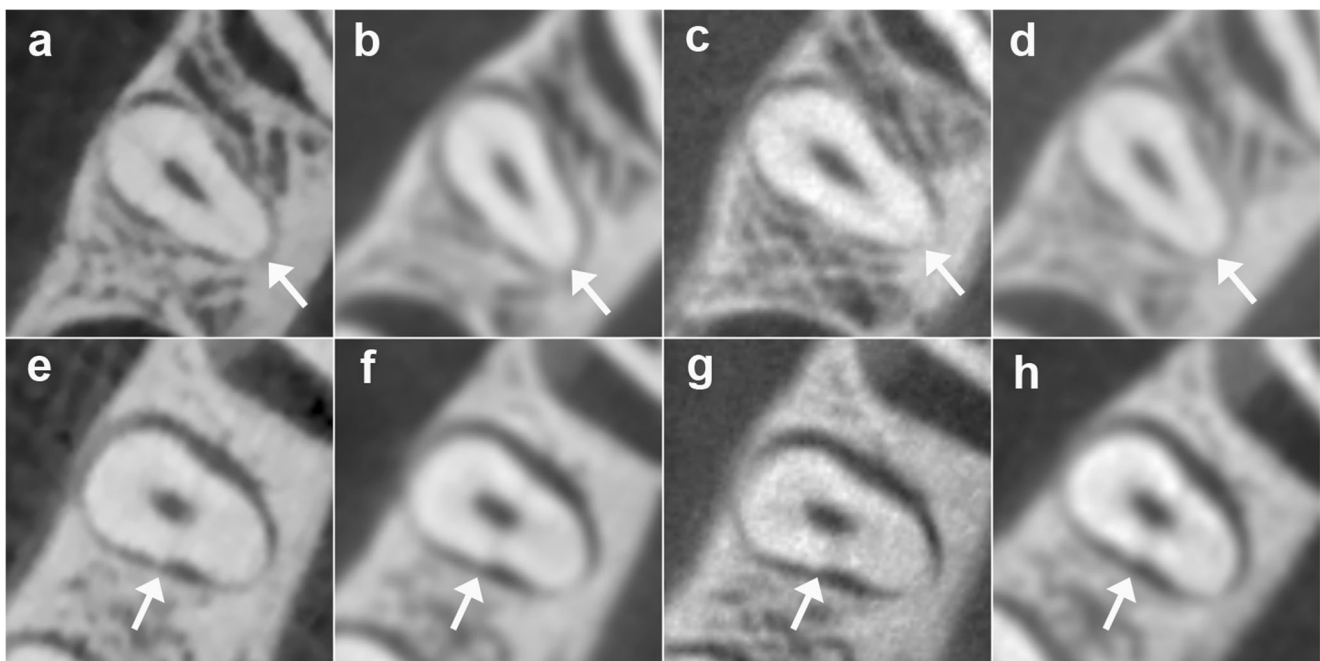


Fig. 2 Example CBCT axial images of one premolar with buccolingual vertical root fracture (a–d) and another premolar with mesiodistal vertical root fracture (e–h) scanned with four CBCT units. a, e Images scanned with NewTom VGi voxel size 125 μm , b, f images scanned with ProMax

3D Mid voxel size 150 μm , c, g images scanned with 3D Accuitomo 170 voxel size 125 μm , and d, h images scanned with i-CAT FLX voxel size 125 μm . The white arrows indicate the fracture lines

Table 3 Sensitivity, specificity, area under the receiver operating characteristic curve (AUC), and *P* values for the four CBCT units tested: comparison of mesiodistal vertical root fractures with buccolingual vertical root fractures

		Observer 1		Observer 2		<i>P</i>
		MD VRFs	BL VRFs	MD VRFs	BL VRFs	
NewTom VGi	Sen	0.90	1.00	1.00	1.00	0.21
	Spe	0.96	0.96	1.00	1.00	
	AUC	0.94	0.99	1.00	1.00	
ProMax 3D Mid	Sen	1.00	1.00	1.00	0.89	0.23
	Spe	0.82	0.82	0.96	0.96	
	AUC	0.98	0.99	0.99	0.93	
3D Accuitomo 170	Sen	0.85	1.00	0.85	1.00	0.02*
	Spe	0.91	0.91	0.95	0.95	
	AUC	0.90	0.99	0.92	0.99	
i-CAT FLX	Sen	0.95	1.00	0.95	1.00	0.23
	Spe	0.92	0.92	0.95	0.95	
	AUC	0.95	0.98	0.96	1.00	

Sen sensitivity, *Spe* specificity, *AUC* area under the receiver operating characteristic curve, *MD* mesiodistal, *BL* buccolingual, *VRF* vertical root fracture

*Significant difference between the mesiodistal and buccolingual VRFs for AUC

operating characteristic curves for the mesiodistal and buccolingual VRFs from the four included CBCT units are shown in Fig. 3.

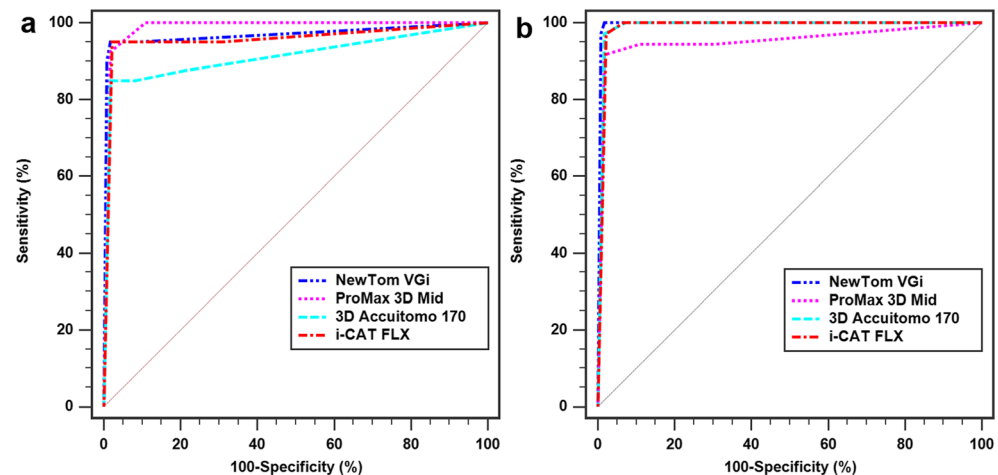
Discussion

Studies on the effect of fracture orientation on the detection accuracy of VRFs using CBCT imaging have been reported previously. However, the VRF in the teeth used in these studies had intra-canal filling materials or metal posts, which may have had an influence on the visualization and detection of fracture lines due to beam hardening effects [13, 28]. Therefore, it is necessary to investigate the effect of fracture orientation in non-endodontically treated teeth. The results from the present study demonstrate that only for CBCT data

from the 3D Accuitomo 170 device the fracture orientation seems to have played a role in the detection accuracy of VRFs.

CBCT can capture structures three-dimensionally. This overcomes the drawbacks such as superimposition from two-dimensional intra-oral radiography, which is why CBCT provides more accurate detection of VRFs than periapical radiography [11, 13]. The present study found that for the CBCT units NewTom VGi, ProMax 3D Mid, and i-CAT FLX, the direction of the fracture line has not had an effect on the detection of VRFs in non-endodontically treated teeth. This is inconsistent with the result reported by Jakobson et al. [13]. In that study, 100 human single-rooted endodontically treated premolars with and without posts inserted into the root canals and VRF in mesiodistal or buccolingual directions were evaluated. The results demonstrated that especially teeth with intra-canal metal posts produced more anatomical and

Fig. 3 Receiver operating characteristic curves for the mesiodistal (a) and buccolingual (b) vertical root fractures from the four CBCT units (data from the two observers combined)



scattering noise in the mesiodistal direction [13]. Though no intra-canal metal posts were used in the present study, the fracture orientation seems to influence the detection of VRFs for the 3D Accuitomo 170 device. This finding is interesting and unexpected. The possible reason may be due to different device and specific image reconstruction algorithms used by the 3D Accuitomo 170 unit for coronal and sagittal images. Nevertheless, this is a mere hypothesis, which needs further evidence to prove and clarify.

To avoid any possible interference from factors other than the fracture orientation, the vertical fracture line was induced with a reproducible and measurable method. In addition, the number of teeth with VRFs in the mesiodistal and buccolingual direction was nearly equal. The overall intra- and inter-observer agreement ranges from moderate to excellent, which seems to exclude any interference from the performance of observers. A possible reason for the ProMax 3D Mid to result in lower intra- and inter-observer agreement scores than the other three units tested may be due to the relatively large FOV and/or voxel size of this specific device [29].

Voxel size and fracture width both have been reported to have an effect on the accuracy of detecting VRFs in non-endodontically treated teeth using CBCT [29]. Therefore, the voxel size corresponding to the highest detection accuracy for each CBCT unit was employed in the present study. To avoid the interference of the voxel size, a 0.125-mm voxel was selected for three of the four CBCT units, and a voxel size of 0.15 mm, which is close to voxel size of 0.125 mm, was selected for the ProMax 3D Mid unit. This difference is most likely not having any influence on the detection accuracy of vertical root fractures [29]. In addition, only the teeth with the same narrow fracture width were used in present study in order to exclude any possible effect from the fracture width.

There are several limitations in the present *in vitro* study. First, the fracture width of teeth with VRFs in the present study may be relatively wider than that of VRFs in patients, which has been reported to vary from 30 to 100 μm [25]. Second, there was no patient movement and artifacts from intra-canal radiopaque materials. Movement during CBCT scanning is very common for the elderly [30, 31], who also are reported to exhibit quite commonly vertical root fractures in non-endodontically treated teeth [2, 5]. Third, clinical symptoms and signs including radiographic features such as secondary bone destruction and widening of the periodontal ligament space along the crack line, which could be helpful in the detection and identification of teeth with VRFs, could not be considered due to the *in vitro* design of the study. Lastly, as information on age and gender related to the origins of the teeth were not available, factors that result in an increase of the mineral density due to intra-tubular sclerosis or root canal narrowing especially in aging patients could not be assessed in this study. As this could be a confounder for the detection of

root fractures, this specific aspect might be worthwhile exploring in future research.

Conclusion

Fracture orientations of teeth with VRFs in non-endodontically treated teeth may have an effect on the detection accuracy using CBCT images, but the effect of fracture orientation seems to be dependent on the CBCT unit used.

Acknowledgements The authors would like to express their sincere thanks to the statistician, Dr. Fang-Chao Liu, for his valuable suggestion on statistical analysis.

Funding The study was supported by National Natural Science Foundation of China (Grant No. 81671034).

Compliance with ethical standards

Conflict of interest The authors declare that they have no conflict of interest.

Ethical approval All procedures performed in studies involving human participants were in accordance with the ethical standards of Institutional Review Board of Peking University School and Hospital of Stomatology (PKUSSIRB-201838111) and with the 1964 Helsinki declaration and its later amendments or comparable ethical standards.

Informed consent For this type of study, formal consent is not required.

References

1. American Association of Endodontists (2008) Endodontics: colleagues for excellence—cracking the cracked tooth code: detection and treatment of various longitudinal tooth fractures. Available at: <https://www.aae.org/specialty/newsletter/cracking-cracked-tooth-code>. Accessed 14 Nov 2018
2. Chan C, Lin C, Tseng S, Jeng J (1999) Vertical root fracture in endodontically versus nonendodontically treated teeth: a survey of 315 cases in Chinese patients. *Oral Surg Oral Med Oral Pathol Oral Radiol Endod* 87:504–507. [https://doi.org/10.1016/S1079-2104\(99\)70252-0](https://doi.org/10.1016/S1079-2104(99)70252-0)
3. Wang P, Yan X, Lui D, Zhang W, Zhang Y, Ma X (2011) Detection of dental root fractures by using cone-beam computed tomography. *Dentomaxillofac Radiol* 40:290–298. <https://doi.org/10.1259/dmfr/84907460>
4. Haueisen H, Gärtner K, Kaiser L, Trohorsch D, Heidemann D (2013) Vertical root fracture: prevalence, etiology, and diagnosis. *Quintessence Int* 44:467–474. <https://doi.org/10.3290/j.qi.a29715>
5. Liao WC, Tsai YL, Wang CY, Chang MC, Huang WL, Lin HJ, Liu HC, Chan CP, Chang SH, Jeng JH (2017) Clinical and radiographic characteristics of vertical root fractures in endodontically and nonendodontically treated teeth. *J Endod* 43:687–693. <https://doi.org/10.1016/j.joen.2016.12.009>
6. Walton RE, Michelich RJ, Smith GN (1984) The histopathogenesis of vertical root fractures. *J Endod* 10:48–56. [https://doi.org/10.1016/S0099-2399\(84\)80037-0](https://doi.org/10.1016/S0099-2399(84)80037-0)

7. Pitts DL, Natkin E (1983) Diagnosis and treatment of vertical root fractures. *J Endod* 9:338–346. [https://doi.org/10.1016/S0099-2399\(83\)80150-2](https://doi.org/10.1016/S0099-2399(83)80150-2)
8. Tsesis I, Beitlitum I, Rosen E (2015) Treatment alternatives for the preservation of vertically root fractured teeth. In: Tamse A, Tsesis I, Rosen E (eds) *Vertical root fractures in dentistry*. Springer, Heidelberg, pp 97–107
9. Walton RE (2017) Vertical root fracture: Factors related to identification. *J Am Dent Assoc* 148:100–105. <https://doi.org/10.1016/j.adaj.2016.11.014>
10. Moule AJ, Kahler B (1999) Diagnosis and management of teeth with vertical root fractures. *Aust Dent J* 44:75–87. <https://doi.org/10.1111/j.1834-7819.1999.tb00205.x>
11. Hassan B, Metska ME, Ozok AR, van der Stelt P, Wesselink PR (2009) Detection of vertical root fractures in endodontically treated teeth by a cone beam computed tomography scan. *J Endod* 35:719–722. <https://doi.org/10.1016/j.joen.2009.01.022>
12. Kambungton J, Janhom A, Prapayasatok S, Pongsiriwet S (2012) Assessment of vertical root fractures using three imaging modalities: cone beam CT, intraoral digital radiography and film. *Dentomaxillofac Radiol* 41:91–95. <https://doi.org/10.1259/dmfr/49798768>
13. Jakobson SJ, Westphalen VP, Silva Neto UX, Fariniuk LF, Schroeder AG, Carneiro E (2014) The influence of metallic posts in the detection of vertical root fractures using different imaging examinations. *Dentomaxillofac Radiol* 43:20130287. <https://doi.org/10.1259/dmfr.20130287>
14. De Martin ESD, Campos CN, Pires Carvalho AC, Devito KL (2018) Diagnosis of mesiodistal vertical root fractures in teeth with metal posts: influence of applying filters in cone-beam computed tomography images at different resolutions. *J Endod* 44:470–474. <https://doi.org/10.1016/j.joen.2017.08.030>
15. Youssefzadeh S, Gahleitner A, Dorffner R, Bernhart T, Kainberger FM (1999) Dental vertical root fractures: value of CT in detection. *Radiology* 210:545–549. <https://doi.org/10.1148/radiology.210.2.r99ja20545>
16. Tsesis I, Kamburoglu K, Katz A, Tamse A, Kaffe I, Kfir A (2008) Comparison of digital with conventional radiography in detection of vertical root fractures in endodontically treated maxillary premolars: an ex vivo study. *Oral Surg Oral Med Oral Pathol Oral Radiol Endod* 106:124–128. <https://doi.org/10.1016/j.tripleo.2007.09.007>
17. Khedmat S, Rouhi N, Drage N, Shokouhinejad N, Nekoofar MH (2012) Evaluation of three imaging techniques for the detection of vertical root fractures in the absence and presence of gutta-percha root fillings. *Int Endod J* 45:1004–1009. <https://doi.org/10.1111/j.1365-2591.2012.02062.x>
18. Kondylidou-Sidira A, Fardi A, Giannopoulou M, Parisi N (2013) Detection of experimentally induced root fractures on digital and conventional radiographs: an in vitro study. *Odontology* 101:89–95. <https://doi.org/10.1007/s10266-012-0059-0>
19. Rud J, Omnell KA (1970) Root fractures due to corrosion. Diagnostic aspects. *Scand J Dent Res* 78:397–403. <https://doi.org/10.1111/j.1600-0722.1970.tb02088.x>
20. Corbella S, Del Fabbro M, Tamse A, Rosen E, Tsesis I, Taschieri S (2014) Cone beam computed tomography for the diagnosis of vertical root fractures: a systematic review of the literature and meta-analysis. *Oral Surg Oral Med Oral Pathol Oral Radiol* 118:593–602. <https://doi.org/10.1016/j.oooo.2014.07.014>
21. Talwar S, Utneja S, Nawal RR, Kaushik A, Srivastava D, Oberoy SS (2016) Role of cone-beam computed tomography in diagnosis of vertical root fractures: a systematic review and meta-analysis. *J Endod* 42:12–24. <https://doi.org/10.1016/j.joen.2015.09.012>
22. Melo SL, Bortoluzzi EA, Abreu M Jr, Correa LR, Correa M (2010) Diagnostic ability of a cone-beam computed tomography scan to assess longitudinal root fractures in prosthetically treated teeth. *J Endod* 36:1879–1882. <https://doi.org/10.1016/j.joen.2010.08.025>
23. Özer SY (2011) Detection of vertical root fractures by using cone beam computed tomography with variable voxel sizes in an in vitro model. *J Endod* 37:75–79. <https://doi.org/10.1016/j.joen.2010.04.021>
24. Melo SL, Haiter-Neto F, Correa LR, Scarfe WC, Farman AG (2013) Comparative diagnostic yield of cone beam CT reconstruction using various software programs on the detection of vertical root fractures. *Dentomaxillofac Radiol* 42:20120459. <https://doi.org/10.1259/dmfr.20120459>
25. Brady E, Mannocci F, Brown J, Wilson R, Patel S (2014) A comparison of cone beam computed tomography and periapical radiography for the detection of vertical root fractures in nonendodontically treated teeth. *Int Endod J* 47:735–746. <https://doi.org/10.1111/iej.12209>
26. Ma RH, Ge ZP, Li G (2016) Detection accuracy of root fractures in cone-beam computed tomography images: a systematic review and meta-analysis. *Int Endod J* 49:646–654. <https://doi.org/10.1111/iej.12490>
27. Zhang ZL, Cheng JG, Li G, Zhang JZ, Zhang ZY, Ma XC (2012) Measurement accuracy of temporomandibular joint space in Promax 3-dimensional cone-beam computerized tomography images. *Oral Surg Oral Med Oral Pathol Oral Radiol* 114:112–117. <https://doi.org/10.1016/j.oooo.2011.11.020>
28. Hassan B, Metska ME, Ozok AR, van der Stelt P, Wesselink PR (2010) Comparison of five cone beam computed tomography systems for the detection of vertical root fractures. *J Endod* 36:126–129. <https://doi.org/10.1016/j.joen.2009.09.013>
29. Guo XL, Li G, Zheng JQ, Ma RH, Liu FC, Yuan FS, Lyu PJ, Guo YJ, Yin S (2019) Accuracy of detecting vertical root fractures in non-root filled teeth using cone beam computed tomography: effect of voxel size and fracture width. *Int Endod J*. <https://doi.org/10.1111/iej.13076>
30. Donaldson K, O'Connor S, Heath N (2013) Dental cone beam CT image quality possibly reduced by patient movement. *Dentomaxillofac Radiol* 42:91866873. <https://doi.org/10.1259/dmfr/91866873>
31. Nardi C, Borri C, Regini F, Calistri L, Castellani A, Lorini C, Colagrande S (2015) Metal and motion artifacts by cone beam computed tomography (CBCT) in dental and maxillofacial study. *Radiol Med* 120:618–626. <https://doi.org/10.1007/s11547-015-0496-2>

Publisher's note Springer Nature remains neutral with regard to jurisdictional claims in published maps and institutional affiliations.